



Published in final edited form as:

JACC Cardiovasc Imaging. 2014 March ; 7(3): 215–224. doi:10.1016/j.jcmg.2013.12.010.

Geometric Characterization of Patient Specific Total Cavopulmonary Connections and Its Relationship to Hemodynamics

Elaine Tang, BEng^{*}, Maria Restrepo, BS[†], Christopher M. Haggerty, PhD[†], Lucia Mirabella, PhD[†], James Bethel, PhD[‡], Kevin K. Whitehead, MD, PhD[§], Mark A. Fogel, MD[§], and Ajit P. Yoganathan, PhD[†]

^{*}School of Chemical and Biomolecular Engineering, Georgia Institute of Technology, Atlanta, GA

[†]Wallace H. Coulter Department of Biomedical Engineering, Georgia Institute of Technology & Emory University, Atlanta, GA

[‡]Westat, Rockville, MD

[§]Division of Cardiology, Children's Hospital of Philadelphia, Philadelphia, PA

Abstract

Total cavopulmonary connection (TCPC) geometries have great variability. Geometric features like diameter, connection angle and distance between vessels, are hypothesized to affect the energetics and flow dynamics within the connection. This study aimed to identify important geometric characteristics that can influence TCPC hemodynamics. Anatomies from 108 consecutive patients were reconstructed from cardiac magnetic resonance images (MRI) and analyzed for their geometric features. Vessel flow rates were computed from phase contrast MRI. Computational fluid dynamics simulations were carried out to quantify the indexed power loss and hepatic flow distribution. TCPC indexed power loss correlated inversely with minimum Fontan pathway (FP), left and right pulmonary arteries diameters. Cardiac index correlated with minimum FP diameter and superior vena cava (SVC) minimum/maximum diameter ratio. Hepatic flow distribution correlated with caval offset, pulmonary flow distribution, and the angle between FP and SVC. These correlations can have important implications on future connection design and patient follow-up.

Keywords

Fontan procedure; congenital heart defects; hemodynamics

© 2014 American College of Cardiology Foundation. Published by Elsevier Inc. All rights reserved.

Address correspondence to: Ajit P. Yoganathan, Associate Chair, Wallace H. Coulter Department of Biomedical Engineering, Georgia Institute of Technology & Emory University, Technology Enterprise Park, Suite 200, 387 Technology Circle, Atlanta, GA 30313-2412, Tel: +1 404-894-2849, Fax: +1 404-385-1268, ajit.yoganathan@bme.gatech.edu.

Publisher's Disclaimer: This is a PDF file of an unedited manuscript that has been accepted for publication. As a service to our customers we are providing this early version of the manuscript. The manuscript will undergo copyediting, typesetting, and review of the resulting proof before it is published in its final citable form. Please note that during the production process errors may be discovered which could affect the content, and all legal disclaimers that apply to the journal pertain.

Disclosures: There are no industry relationships to disclose.

Introduction

The Fontan procedure is a palliative surgical technique for single ventricle patients. The resulting total cavopulmonary connection (TCPC) is completed by routing superior and inferior vena cava (SVC and IVC) flow directly to the left and right pulmonary arteries (LPA and RPA), bypassing the right heart. This procedure improves life expectancy, however, many patients remain at risk for long-term complications which may be attributed to unfavorable hemodynamics. For example, there is evidence to show a possible link between TCPC energy dissipation and exercise tolerance (1). As another example, pulmonary arteriovenous malformations (PAVM) can be palliated by avoiding unbalanced distribution of hepatic blood flow between the lungs (2). Because of complex native vessel morphology and difference in surgical techniques, a great variability exists in the TCPC geometry. The intra-atrial pathway usually forms a bulge, which promotes flow mixing within the Fontan pathway (FP) while the extracardiac conduit has more uniform cross sectional area which results in a more streamlined flow. Such variability can in turn translate to differences in connection flow dynamics.

The hypothesis of this study is that significant correlations exist between certain TCPC geometric features and hemodynamics such as power loss, cardiac index and flow distributions. This work aims to provide further insight to surgeons and cardiologists regarding the connection geometries to avoid, and also help in the interpretation of suboptimal hemodynamics relative to the post-operative geometries.

Methods

Patient Cohort

One hundred and thirty one consecutive single ventricle patients with a TCPC were selected from the Georgia Tech–Children’s Hospital of Philadelphia Fontan database. Prospective cardiac magnetic resonance (CMR) data was acquired between 2002 and 2012. The study was approved by the institutional review boards (IRB) of both institutions. Patient data were collected with informed consent. Cases with severe CMR artifacts, diagnosis of Ebstein’s anomaly, atriopulmonary connections, left SVC (LSVC) to coronary sinus to systemic venous pathway connection, and bifurcated Fontan Y-graft were excluded. A total of 108 patients were included (Table 1).

Image Reconstruction and Hemodynamic Assessment

Steady-state free precession vectorcardiogram gated CMR images were acquired in the transverse plane using a Siemens Avanto 1.5 Tesla whole-body magnetic resonance imaging scanner (Siemens Medical Systems, Malvern, PA) (Table 2). The CMR images were acquired with 3 excitations every other heartbeat at end-diastole. In general, smaller voxel sizes were chosen for smaller patients to accurately resolve first and second order pulmonary arterial branching. To compensate for the decreased signal-to-noise loss, one to two additional excitations were added and over-sampling was increased to 50%. The images were interpolated and segmented to select the TCPC anatomies using a previously developed and validated methodology (3).

Phase contrast magnetic resonance imaging (PC-MRI) was utilized to acquire through-plane velocity profiles across the aortic valve, the vena cavae, LPA and RPA over the cardiac cycle under breath-hold conditions. Vessel flow rates were time-averaged and used to compute cardiac index (CI) and pulmonary flow distribution (PFD). They were also used as time-averaged flow boundary conditions for computational fluid dynamics (CFD) simulations to compute connection indexed power loss (iPL) and hepatic flow distribution

(HFD) (Figure 1). The velocity segmentation and CFD methodology have been previously described (2).

Geometric Analysis

Vascular Modeling ToolKit (www.vmtk.org) was used to compute vessel centerlines and bifurcation vectors (which contain the location and direction of the point which the centerline bifurcates into branches). Each point of the centerline represents the 3-dimensional (3D) coordinates of the center of the maximum sphere inscribed in the vessel lumen at that point, equipped with the radius of such sphere (Figure 2). Geometric parameters analyzed include vessel diameter, minimum/maximum diameter ratio (to observe any vessel narrowing), relative LPA area (comparing the relative size of LPA and RPA cross sections), vessel offsets and connection angles (Figure 3). To account for difference in patient size, vessel diameters were normalized by the square root of body surface area ($\sqrt{\text{BSA}}$ [m]). Vessel offsets were normalized by mean FP diameter of each patient instead of BSA.

Statistical Analysis

Statistical analysis was performed using IBM SPSS Statistics (version 20, IBM Corporation, Armonk, New York). Paired-samples t-test (or Wilcoxon signed-rank test) and repeated-measures ANOVA (or Friedman test) were used to compare geometric parameters among vessel types (normality tested by Shapiro-Wilk test). Pearson's correlation was performed first to identify trends between the geometric and hemodynamic variables. The significant variables were selected, and multiple linear regression (MLR) of the hemodynamic endpoints was performed using forward stepwise procedures. P-value 0.05 was considered significant (two-tailed). All models were screened for outliers (standardized residual not within ± 2) and influential observations (Cook's distance > 0.04). Skewness was quantified using SPSS. Outliers and influential observations were reviewed and all calculations were verified.

Geometric and Hemodynamic Characterization

The average geometric features of 108 TCPC are presented in Table 3. FP had the largest average diameter compared to other vessels ($p < 0.001$). Comparing the PAs, LPA diameters were smaller than the RPA on average (minimum diameters: $p < 0.001$; mean diameters: $p < 0.001$; maximum diameters: $p = 0.02$). Of particular note is the lower minimum/maximum diameter ratio at the LPA ($p < 0.001$), implying the diameter was less uniform than the RPA and different degrees of vessel narrowing were observed.

For cases without LSVC and azygos vein (AZ), ($N = 92$), the SVC anastomosis was generally more symmetric with respect to the PAs, demonstrated by similar SVC-LPA and SVC-RPA angles ($p = 0.566$) while the FP-LPA angle was significantly larger than FP-RPA angle ($p < 0.001$). Hemodynamic findings from flow and CFD analysis are presented in Table 3. There were significant correlations between PFD and HFD ($r = 0.396$, $p < 0.001$) and between CI and the natural logarithm of iPL ($r = -0.366$, $p < 0.001$).

Correlation between Geometry and Hemodynamics

Significant correlations between geometric variables and hemodynamic metrics were observed. Due to the skewness of the offset magnitude data (skewness = 3.96 ± 0.23), 4 cases with discrete caval offset magnitude (Figure 4) were excluded in subsequent statistical correlations, resulting in $N = 104$ (skewness = 1.17 ± 0.24).

Indexed Power Loss (iPL) and Cardiac Index (CI)

By curve fitting, a power law relationship between iPL and normalized vessel diameter was observed (Figure 5). Therefore, the normalized diameters were transformed to its respective exponent (e.g. normalized minimum FP diameter was powered with -2.274) for MLR. From MLR, only normalized minimum vessel diameters of FP, LPA and RPA were identified as independent predictors. The strongest predictor was normalized minimum FP diameter, which was the vessel that carried the majority of TCPC blood ($59\pm 15\%$ of total systemic return on average). In addition, the majority of patients with low minimum FP diameter in this cohort had an intra-atrial connection (Figure 5). Among the PAs, LPA (smaller diameter on average) was a more significant predictor.

Consistent with the trend between iPL and CI, and between iPL and minimum FP diameter, significant positive correlation between CI and normalized minimum FP diameter was observed (standard coefficient= 0.347 ; $r=0.355$, $p<0.001$). Also, positive significant correlation between CI and SVC minimum/maximum diameter ratio (standard coefficient= 0.215 ; $r=0.229$, $p=0.02$) was observed.

Hepatic and Pulmonary Flow Distribution

To exclude the influence of additional vessels, correlations of %HFD(LPA) were carried out only on cases with the four typical TCPC vessels (FP, SVC, LPA and RPA; $N=90$). Normalized caval offset with SVC correlated most significantly with %HFD(LPA) (Figure 6). When the FP was connected to the left relative to the SVC, higher flow from the FP coursed through the LPA than the RPA due to proximity. Significant positive correlation was found between %HFD(LPA) and %PFD(LPA) in this subset of patients (Figure 6). Also, significant correlations were found between %HFD(LPA) and FP-SVC angle (Figure 6). An example showing the influence of FP-SVC angle on %HFD(LPA) is illustrated by Figure 7.

For %PFD(LPA), it was found by MLR that relative LPA area was the only independent predictor (Figure 8).

All MLR findings were further evaluated by including the outliers into the MLR of ranked ordinal dependent variables (ranked iPL, ranked HFD, etc.) and ranked caval offset (with SVC) as a confirmatory analysis using non-parametric methods. Even after including the outliers in the MLR, the same parameters were still identified as significant, which further confirmed the findings.

Discussion

Impact of Geometry on Energy Dissipation

Geometric alterations of TCPC to minimize energy dissipation have been widely studied in idealized geometries. Earlier studies have emphasized the benefit of having caval offsets to reduce caval flow collision hence lower TCPC power loss. Using patient specific geometry, Dasi et. al. (4) has shown there existed a strong inverse correlation between minimum PA area and TCPC energy dissipation ($N=22$). While these findings have provided significant insights, investigations to compare the relative importance of different geometric parameters are still lacking.

In this cohort, the effect of minimum vessel size manifested as the most important geometric parameter. Even when the average LPA diameter was smaller than that of the FP, the correlation between minimum FP diameter and iPL was the most significant. This could be because FP carried higher blood flow, which further elevated energy loss when the diameter

was small. On the other hand, caval offset was not significantly correlated to iPL in this cohort, in spite of previous findings. This indicates that it may not be of critical importance compared to vessel diameter in order to minimize power loss.

Though it was not clear what caused the narrowing of the TCPC vessels, these findings suggested it may be important to dilate the narrowing, or to utilize strategies to promote vessel growth, especially in intra-atrial patients. This is confirmed also by the negative correlation between CI and minimum FP diameter. Long term post-operative follow-up is essential and a study evaluating the physiological outcomes after intervention by stent implantation may be warranted, as the pathway narrowing can potentially elevate energy loss during high cardiac flow and lead to exercise intolerance in these patients (1).

Factors Affecting Hepatic Flow Distribution

Avoiding unbalanced distribution of hepatic flow to both lungs has been shown to be important for palliation of PAVM in single ventricle patients (2). Dasi et al. has shown that %HFD(LPA) was strongly correlated with caval offset in extracardiac patients (N=5), and with %PFD(LPA) in intra-atrial patients (N=5) (5). In this cohort as a whole, %HFD(LPA) was most significantly correlated with normalized caval offset (with SVC), which agreed with the previous study. This emphasizes again the need to consider the relative displacement between FP and SVC in the staged procedures.

Another significant variable for HFD is the FP-SVC angle. From the cohort characterization, FP was generally connected towards the left (FP-LPA angle > FP-RPA angle) favoring HFD to the LPA; this was not the case with SVC (SVC-LPA angle \approx SVC-RPA angle). When the FP-SVC angle was large (close to 180°), the FP and SVC flows were directly opposed and subjected to collisions. This likely resulted in more recirculation, negating the preference of the FP flow towards the LPA. From Figure 7, both cases had low caval offset magnitudes and FP pointing towards the left, but (a) was connected anteriorly towards the PAs. On the other hand, (b) had large FP-SVC angle that almost resembled a straight pipe. Therefore, FP and SVC blood collided and mixed before leaving the PAs, resulting in low %HFD(LPA).

These findings suggest that while caval offset remains the most important geometric determinant of HFD, in cases where caval offset is constrained (e.g. by surrounding structures) and pulmonary flow distribution is unbalanced, FP should be angled not only towards the desired side of the lungs (left or right, based on a patient specific circumstance). The relative angle with the SVC should be considered to avoid head on collisions and reduce caval flow mixing.

While this cohort included patients with various geometric features, it should be noted that the above findings are only applicable for typical TCPC (SVC, (LSVC) and FP are directly connected to the PAs) with low caval offset. For more complex configurations like the bifurcated Fontan Y-graft, additional parameters may have to be included. In addition, while this manuscript has established correlations between TCPC geometric parameters and hemodynamic surrogates like iPL and HFD, clinical importance of iPL on patient outcome still warrants further investigations.

Limitations

CMR spatial resolution could affect accuracy of the reconstructed vessel sizes. The 3D reconstruction method used for transverse CMR data was validated with TCPC geometry, with 0.96% error for PA diameter measurement and 1.77% error on radius curvature (3). The in-plane resolution for PC-MRI data ranged from 0.547–1.875mm, which is still sufficient for this analysis, considering the diameter of the right upper lobe PA ranged from

4–9mm. However in cases with PA stenosis, the sparse transverse slices could potentially lead to inaccuracies in the PA diameter.

4D (3D in time) PC-MRI acquisition would have allowed for the assessment of *in vivo* hemodynamics; because of patient scan time limitations imposed by the IRB, this was not performed. CFD assessment was an approximation to the physiology as it applied time-averaged boundary conditions and assumed rigid vessel wall. PC-MRI data was acquired under breath-hold condition to reduce scan time, which ignored the physiologic variability with respiration. Posture, exertion etc, can also affect the hemodynamics. Aortopulmonary collateral flow, calculated as the difference between cardiac output and systemic return, was 0.40 ± 0.84 L/min in this cohort ($8\% \pm 20\%$ of cardiac output). Collateral flow and fenestrations were ignored in the simulations, which might have an influence on the hemodynamics.

Acknowledgments

This study was supported by the National Heart, Lung, and Blood Institute Grants HL67622 and HL098252.

Abbreviation List

TCPC	total cavopulmonary connection
CFD	computational fluid dynamics
CMR	cardiac magnetic resonance
(I/S)VC	inferior/superior vena cava
FP	Fontan pathway, which contains the native IVC tissue along with intra-atrial pathway or extracardiac conduit
(L/R)PA	left/right pulmonary artery
BSA	body surface area
iPL	indexed power loss
HFD	hepatic flow distribution

References

1. Whitehead KK, Pekkan K, Kitajima HD, Paridon SM, Yoganathan AP, Fogel MA. Nonlinear power loss during exercise in single-ventricle patients after the Fontan: insights from computational fluid dynamics. *Circulation*. 2007; 116:1165–1171. [PubMed: 17846299]
2. Sundareswaran K, de Zélicourt D, Sharma S, et al. Correction of pulmonary arteriovenous malformation using image based surgical planning. *JACC Imaging*. 2009; 2:1024–1030.
3. Frakes DH, Smith MJ, Parks J, Sharma S, Fogel M, Yoganathan AP. New techniques for the reconstruction of complex vascular anatomies from MRI images. *J Cardiovasc Magn Reson*. 2005; 7:425–432. [PubMed: 15881525]
4. Dasi LP, Krishnankuttyrema R, Kitajima HD, et al. Fontan hemodynamics: importance of pulmonary artery diameter. *J Thorac Cardiovasc Surg*. 2009; 137:560–564. [PubMed: 19258065]
5. Dasi LP, Whitehead K, Pekkan K, et al. Pulmonary hepatic flow distribution in total cavopulmonary connections: Extracardiac versus intracardiac. *J Thorac Cardiovasc Surg*. 2011; 141:207–214. [PubMed: 20621314]

Flow Analysis

- **Cardiac Index (CI)** = $\frac{\text{Cardiac Output [CO, } \frac{L}{\text{min}}]}{\text{BSA [m}^2]}$
- **%PFD(LPA)** = $\frac{(\text{LPA flow})}{(\text{LPA flow}) + (\text{RPA flow})} \times 100\%$

Computational Fluid Dynamics Analysis

- **Indexed Power Loss (iPL)**

$$iPL = \frac{\dot{E}_{Loss}}{\rho Q^3 / BSA^2} \quad \dot{E}_{Loss} = \sum_{\text{inlets } A} \int \left(p + \frac{1}{2} \rho v^2 \right) v \cdot dA - \sum_{\text{outlets } A} \int \left(p + \frac{1}{2} \rho v^2 \right) v \cdot dA$$

p = static pressure relative to the FP measured from CFD

(pressure difference between the specified vessel and FP);

Q = total systemic return; v = velocity; ρ = blood density (1060 kg m⁻³);

A = cross sectional area of the inlet/outlet; BSA = body surface area

inlets = IVC, SVC, LSVC or AZ; outlets = LPA, RPA or RUPA

- **%HFD(LPA)** = $\frac{\text{Hepatic flow to left lung}}{\text{Total hepatic flow}} \times 100\%$

Figure 1. Definitions of hemodynamic parameters analyzed

Definitions of hemodynamic parameters obtained from PC-MRI flow analysis (cardiac index and pulmonary flow distribution), and from computational fluid dynamics analysis (indexed power loss and hepatic flow distribution).

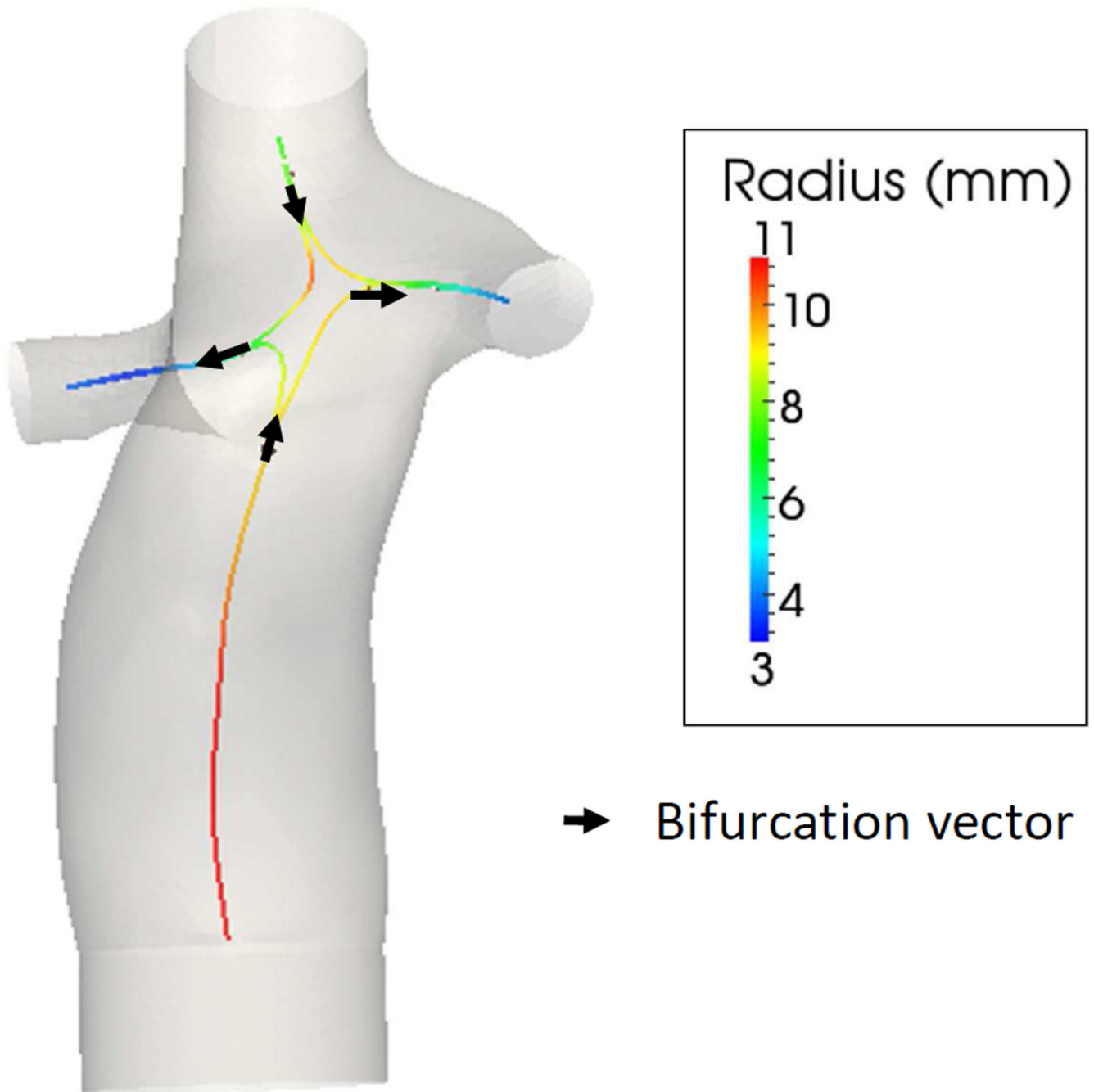


Figure 2. Example of vessel centerlines and bifurcation vectors

An example of a TCPC anatomy with vessel centerlines color-coded by the vessel radius and bifurcation vectors (arrows), both computed with the Vascular Modeling ToolKit (www.vmtk.org).

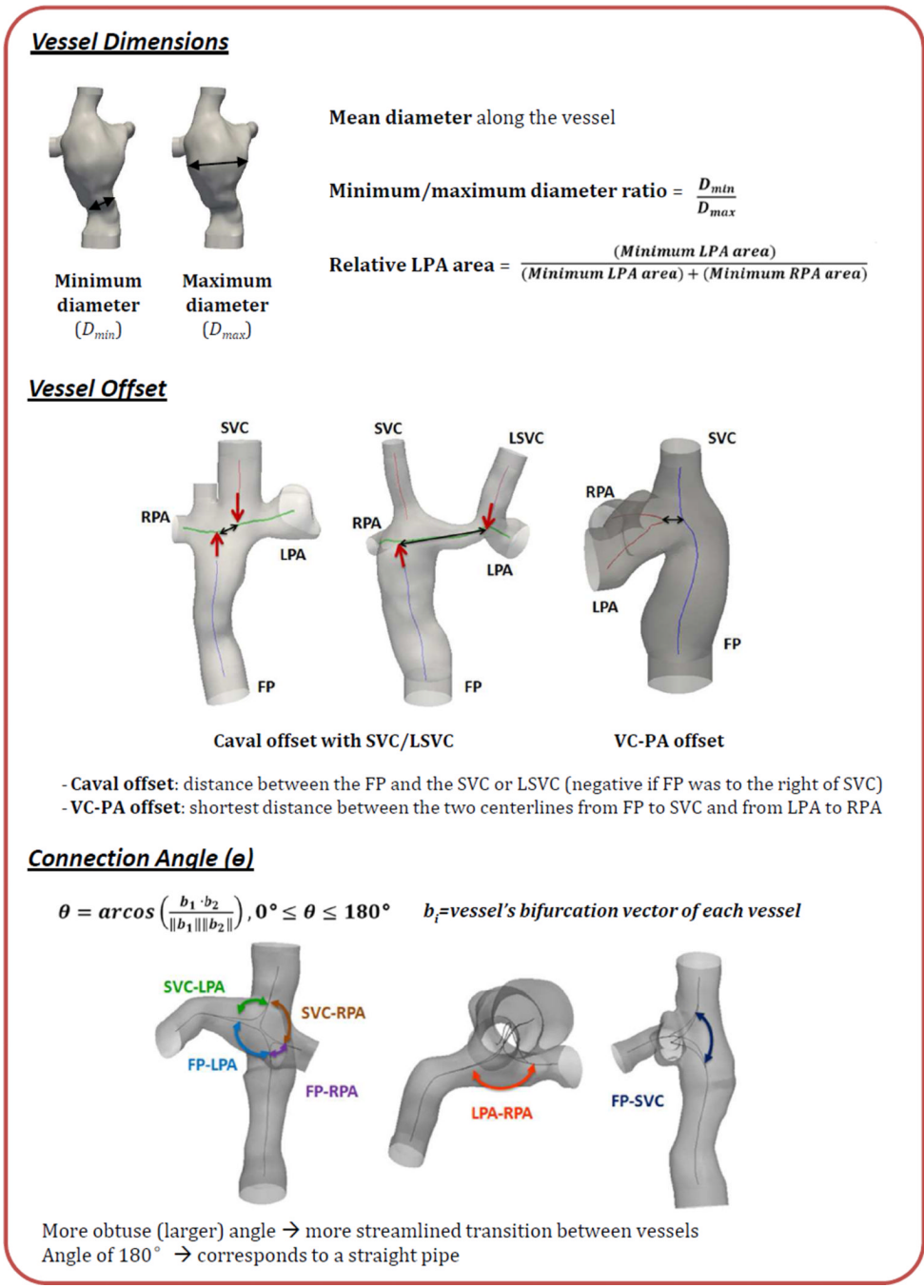


Figure 3. Definitions of geometric parameters analyzed
Definition and illustration of each geometric parameter analyzed.

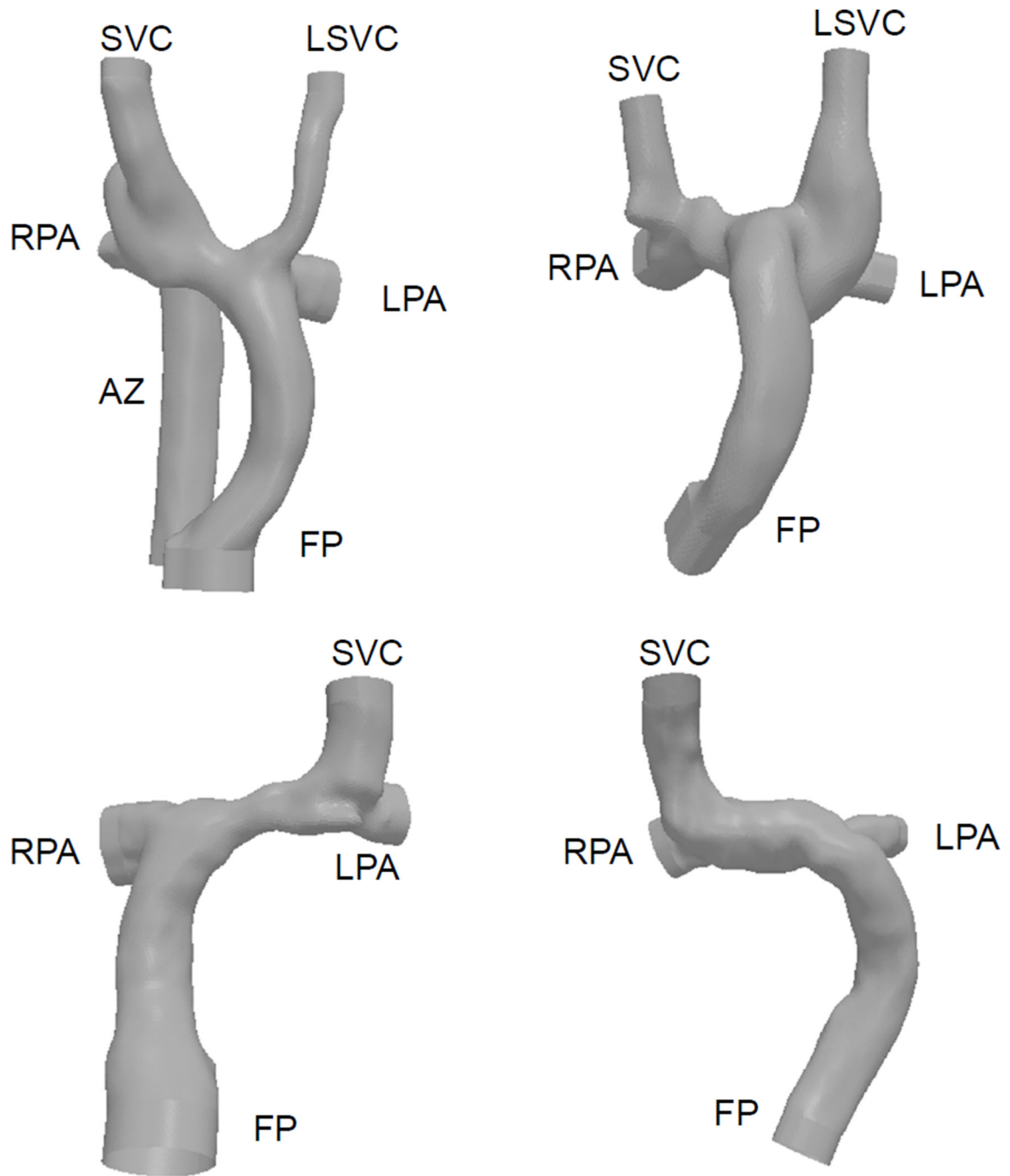


Figure 4. Outlier cases of caval offset magnitude
Anatomies of the 4 outliers of caval offset magnitude excluded from the multiple linear regression analysis.

Multiple regression of iPL (N = 104; R² adjusted = 0.670)

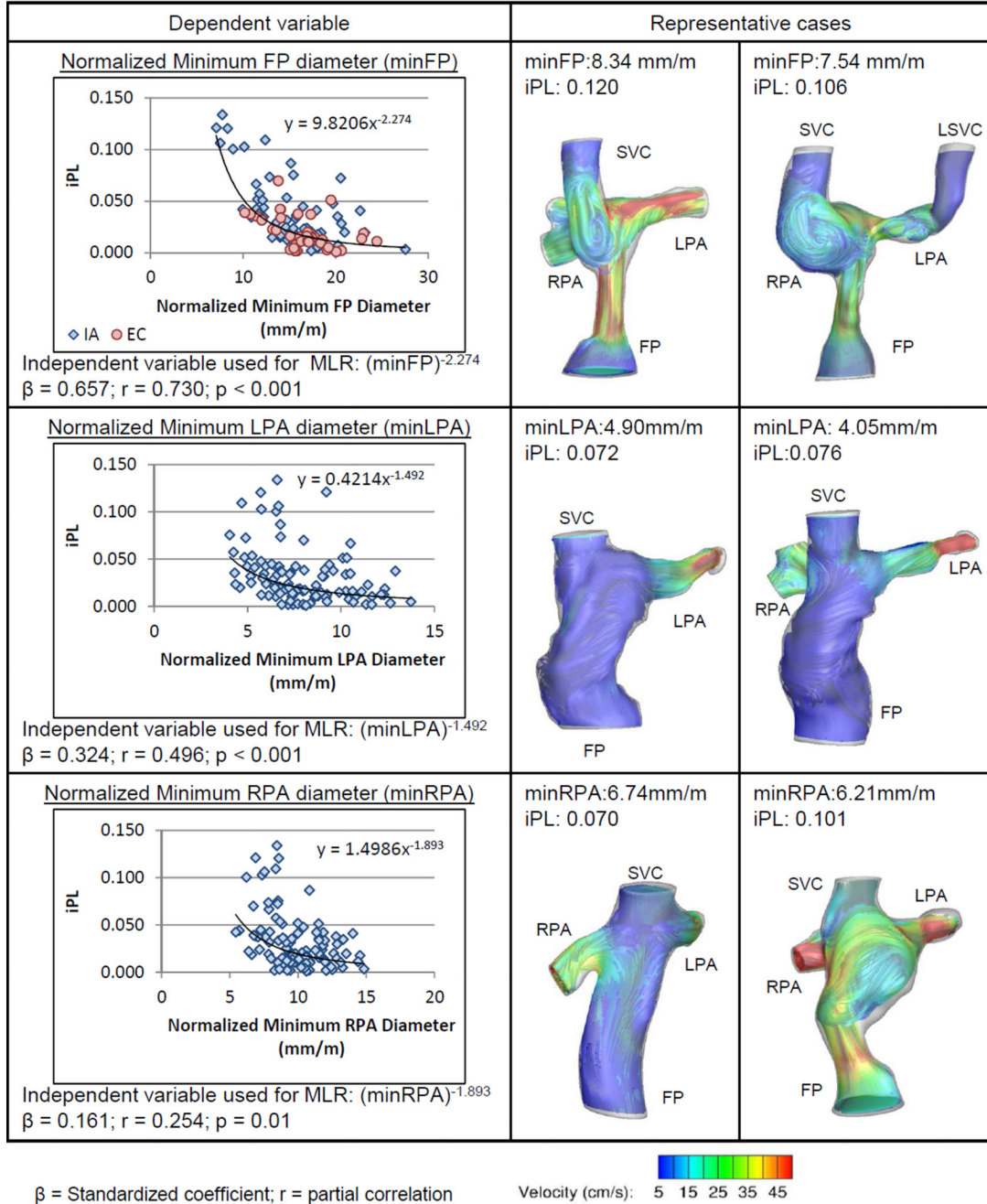
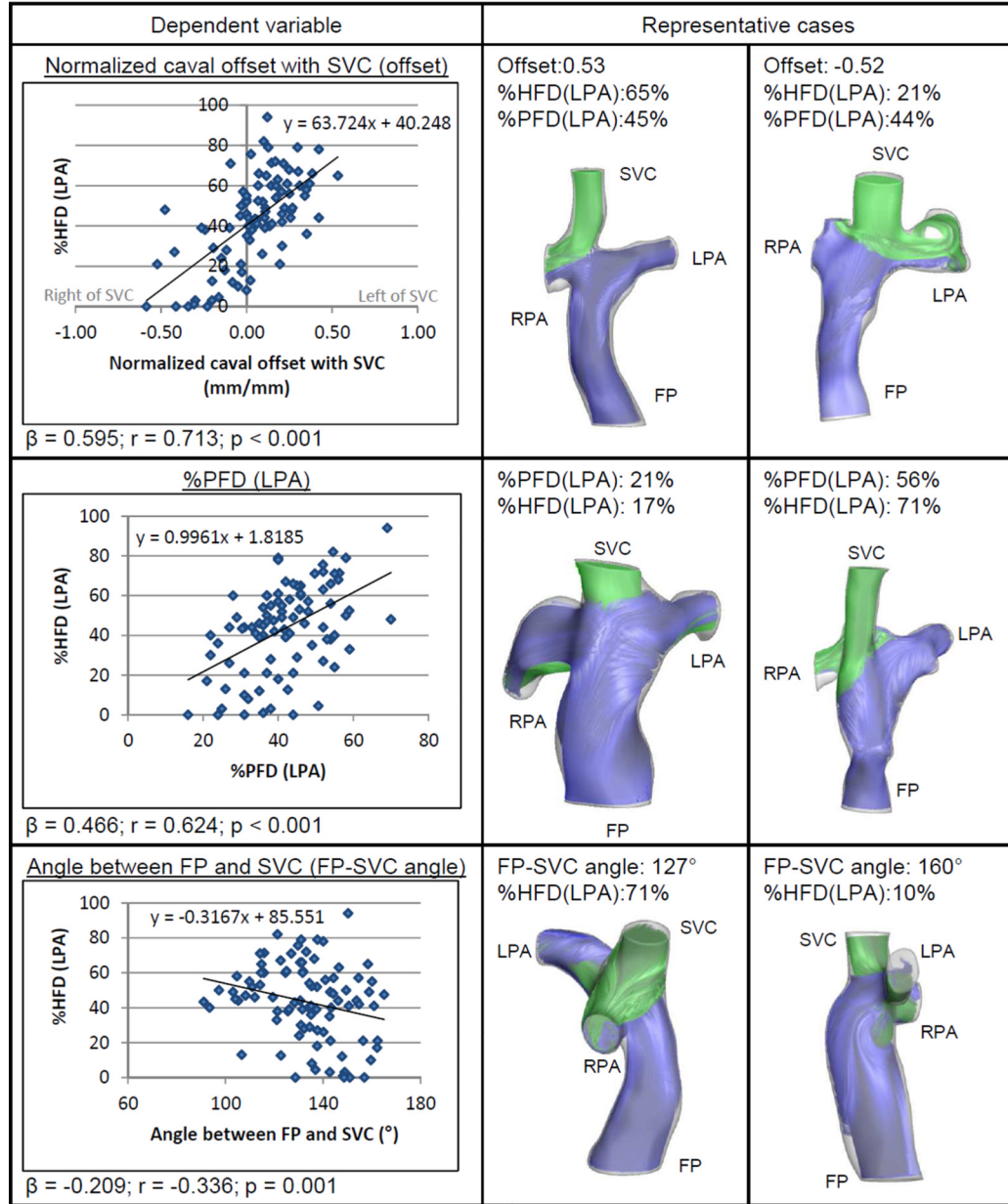


Figure 5. Significant correlations between iPL with normalized minimum FP, LPA and RPA diameters and representative cases for each independent predictor
 Multiple linear regression results show that normalized minimum FP, LPA and RPA diameters are significant independent predictors of iPL. Scatter plots show the inverse relationship between iPL and minimum vessel diameters. Each independent predictor is represented by two patient anatomies with stream traces color-coded by velocity magnitude.

Multiple regression of %HFD(LPA) (N = 90; R² adjusted = 0.649)



β = Standardized coefficient; r = partial correlation;
Green: flow originated from SVC; Blue: flow originated from FP

Figure 6. Significant correlations between %HFD (LPA) with normalized caval offset, %PFD (LPA) and FP-SVC angle and representative cases for each independent predictor
Multiple linear regression results show that normalized caval offset with SVC, %PFD (LPA), FP-SVC angle are significant independent predictors of %HFD (LPA). Scatter plots show the correlations between %HFD (LPA) and each independent predictor. Each independent predictor is represented by two patient anatomies with stream traces color-coded by the vessel of origin.

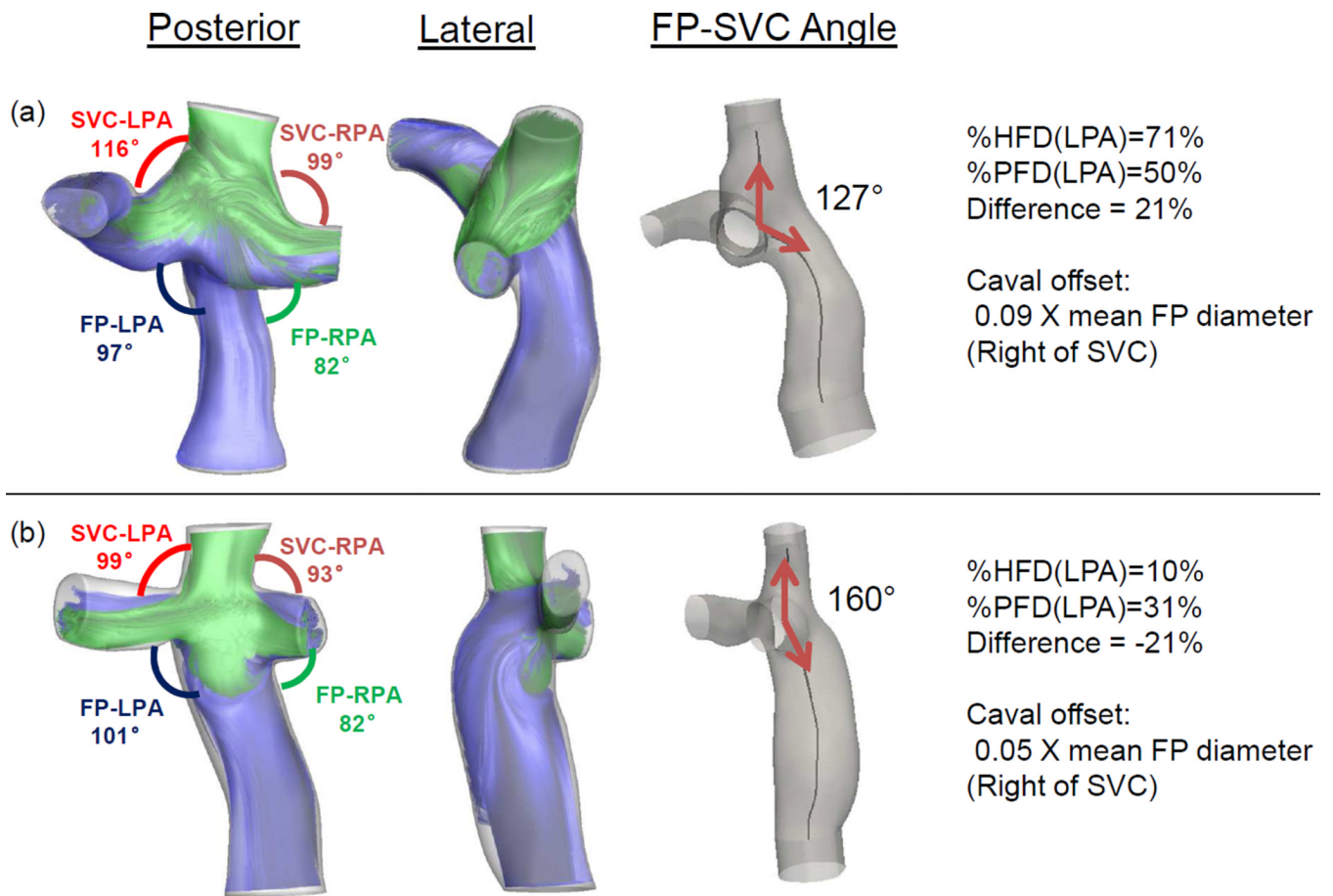
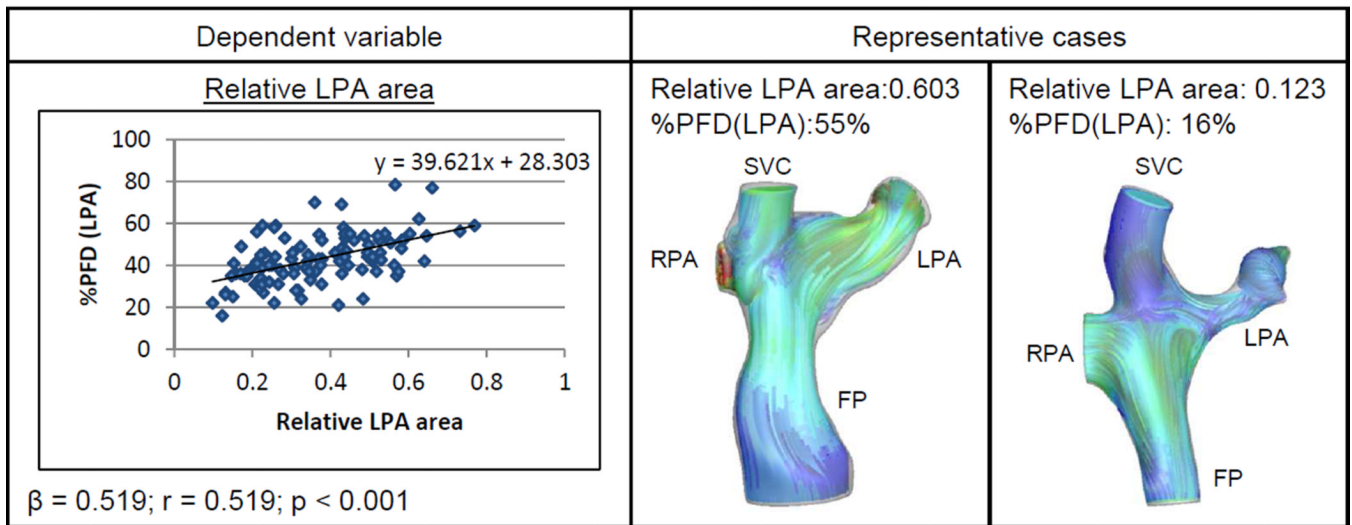


Figure 7. Angulation of FP away from SVC prevents recirculations at the FP-SVC junction
 Examples of two patient anatomies with low (a) and high (b) FP-SVC angle are shown. Both cases had low caval offset magnitudes and FP pointing towards the left, but had different hepatic flow streaming characteristics.

Multiple regression of %PFD(LPA) (N = 104)



β = Standardized coefficient; r = partial correlation


Velocity (cm/s):  5 15 25 35 45

Figure 8. Significant correlation between %PFD (LPA) with relative LPA area
 Multiple linear regression results show that relative LPA area is the only significant independent predictor of %PFD (LPA). Scatter plot shows the trend between %PFD(LPA) and relative LPA area. Two representative patient anatomies with stream traces color-coded by velocity magnitude are presented.

Table 1

Patient cohort summary

Patient Characteristics	Mean \pm standard deviation
Age (years)	10.2 \pm 6.8
Time of scan after Fontan operation (years)*	7.7 \pm 6.9
Body Surface Area (m ²)	1.12 \pm 0.45
Gender (M/F)	63/45
IVC Connection Type (IA/EC) †	67/41
HLHS vs. non-HLHS ‡	40/68

* Data available for 70 patients

† IA – Intra-atrial, EC- Extracardiac

‡ HLHS- Hypoplastic Left Heart Syndrome

Table 2

Summary of CMR parameters

Transverse CMR	Sequence	Steady-state free precession (SSFP)
	No. of slices	30 – 65
	Matrix (pixel)	84 – 256 X 128 – 384
	Spatial resolution (mm)	0.547 – 1.875
	Slice thickness (mm)	3 – 5
	Echo time (ms)	1.10 – 1.96
PC-MRI	Encoding velocity (cm/s)	60 – 150*
	No. of phases	13 – 30

* As low as 60 cm/sec for venous structures and the PAs, and as high as 150 cm/sec for the aorta

Table 3
Cohort geometric characteristics and hemodynamics (mean ± standard deviation)

	FP	SVC	LPA	RPA	RUPA* (N=36)	LSVC† (N=15)	AZ (N=5)	
Normalized vessel diameter (mm/m)	Minimum	15.4 ± 3.8	12.4 ± 2.6	8.0 ± 2.2	10.0 ± 2.1	6.3 ± 1.4	8.8 ± 1.4	
	Mean	18.2 ± 3.8	14.1 ± 2.7	11.0 ± 2.2	12.0 ± 2.2	7.6 ± 1.9	10.7 ± 2.1	
	Maximum	21.5 ± 3.6	16.5 ± 3.0	16.4 ± 3.9	15.6 ± 3.5	9.7 ± 3.4	14.2 ± 1.3	
Minimum/maximum diameter ratio (mm/mm)	0.72 ± 0.12	0.76 ± 0.12	0.51 ± 0.18	0.66 ± 0.16	0.70 ± 0.20	0.73 ± 0.14	0.62 ± 0.10	
Vessel offset (normalized by mean FP diameter)	With SVC							
	Offset	Magnitude	VC-PA	With LSVC (N=15) † Magnitude				
Angle between vessels (degrees)	0.08 ± 0.43		0.24 ± 0.36	0.25 ± 0.22				1.86 ± 0.83
	FP-LPA	FP-RPA	SVC-LPA	SVC-RPA	FP-SVC	LPA-RPA		
Angle between vessels (degrees) (N=15) †	109 ± 16	87 ± 15	106 ± 15	100 ± 15	133 ± 19	108 ± 27		
	LSVC-SVC	LSVC-FP	LSVC-LPA	LSVC-RPA				
Hemodynamics	57 ± 22		131 ± 19	103 ± 19	125 ± 17			
	Cardiac Index (L/min/m ²)		iPL	%PFD(LPA)	%HFD(LPA)			
3.55 ± 0.97		0.031 ± 0.028	43 ± 12	42 ± 22				

* RUPA = Upper lobe of right pulmonary artery

† Among these patients, 4 also have Azygos vein